Ultrasensitive Transverse Magneto-optical Kerr Effect Measurements by means of effective polarization change detection

E. Oblak[1], P. Riego[1,2], L. Fallarino[1], A. Martínez-de-Guerenu[3], F. Arizti[3], A. Berger[1]
[1]CIC nanoGUNE, E-20018 Donostia-San Sebastian, Spain
[2]Departamento de Física de la Materia Condensada, Universidad del País Vasco, UPV/EHU, 48080 Bilbao, Spain
[3]CEIT and Tecnun (University of Navara), E-20018 Donostia-San Sebastian, Spain

Abstract

We perform a detailed comparative study of conventional transverse magneto-optical Kerr effect (T-MOKE) measurements and a methodology that utilizes an effective polarization detection scheme for mixed s- and p-polarized incoming light. To test the ultimate sensitivity of both methods, we also design a series of specialized samples, in which the T-MOKE signal of a Co-film is artificially reduced by means of a Ag overcoat of varying thickness. We find that the effective polarization detection scheme leads to a more than 30-fold increase of the T-MOKE signal and signal-to-noise ratio, even under general operation conditions, which were not individually optimized. This allowed for the observation of T-MOKE hysteresis loops of Co-films that were buried under 80 nm of Ag, for which the MOKE-signal was only 1/600 of that for an uncoated Co-film. In comparison, conventional T-MOKE measurements did not succeed for Ag overcoats thicker than 40 nm.

Introduction

The magneto-optical Kerr effect (MOKE) is a well-established method for the study of magnetization properties of thin films and surfaces [1]. It is based upon small, magnetization induced changes in the optical properties of the material under investigation, which in turn modify the polarization and/or intensity of reflected light [1]. Many aspects of the magneto-optical response of magnetic materials are well understood and there has been a large number of published works over the past decades, in which MOKE was utilized or in which MOKE itself was the subject of investigation [2–12].

Conventionally, the Kerr effect is classified according to the magnetization orientation in reference to the sample surface and the plane-of-incidence: When the magnetization is perpendicular to the sample plane, the effect is called polar MOKE. When the magnetization is in the sample plane, the effect is called longitudinal-MOKE or transverse-MOKE, with the former referring to the magnetization lying in the plane of incidence, and the latter perpendicular to it [4]. Depending on the specific magnetization orientation, the magnetic material affects different aspects of the reflected light. In the case of polar and longitudinal MOKE, the sample magnetization leads to a rotation and ellipticity change of the reflected light polarization that inverts if the magnetization itself is inverted. In the transverse geometry, one observes in general a change in the intensity of the reflected light for incident p-polarized radiation upon magnetization reversal [1, 4, 13]. In addition, there are magneto-optical effects that depend on the magnetization vector in higher order, which are also well described in the literature [14–17]. For most ferromagnetic materials, magneto-optical effects, even the first order MOKE, are rather weak and lead only to a small change in the reflected light. However, they can be measured with a high degree of sensitivity, because the magnetically induced light change can be altered by applying a suitable magnetic field sequence. Thus, very sensitive measurements, even on single atomic layers have been viable [5, 7]. Hereby, studies using the polar or longitudinal MOKE are far more common and overall preferred by the research community, due to the fact that polarization measurements generally allow for a more sensitive detection, even if transverse

MOKE experiments are simpler, given that they are mere intensity measurements.

In addition to materials characterization, magneto-optical effects have found a wide range of applications, as for example, in optical isolation, data-storage technologies, optical modulators, switches and bio-sensing [18–21]. For many applications, it is important to enhance the magneto-optical response [22] and for this reason, numerous studies have been conducted in order to find pathways, in which to enhance magneto-optical effects [3, 22–25]. This is especially significant for transverse MOKE (T-MOKE) applications, because its simple operation is particularly suitable for applications, while on the other hand it also tends to produce rather weak signal amplitudes, if compared to longitudinal and especially polar MOKE [26–28]. Correspondingly, T-MOKE concepts were recently proposed to combine nano-optics and plasmonics with magneto-optical materials [24, 29–31], in which nano-scale and plasmonic effects were capable of enhancing T-MOKE signals or even giving rise to new magneto-optical effects [22]. Hereby, the increase of T-MOKE signals was achieved by fabrication of sophisticated structures, i.e. magneto-optical nanostructured materials such as magnetoplasmonic crystals [24] and multilayered or multi-reflection structures [28].

Despite the wide variety of approaches that have been pursued toward improving T-MOKE sensitivities, a common theme emerges in that the geometric and spectroscopic modifications essentially lead to a reduction of the light amplitude that does not carry magnetic information, so that a relative enhancement of the magnetic change due to T-MOKE can be achieved. This is a sensible strategy even if the associated sample fabrication might be complicated or costly and its application range limited to each specific target application. Thus, it is a most meaningful question, if there is not a more general approach, by which T-MOKE sensitivities can be enhanced. In fact, there are a number of reports, in which effective T-MOKE polarization measurements are described, that achieve a generally enhanced signal level by mixing s- and p-polarized light in the incoming beam [32–34]. However, no comparative study of this measurement scheme has been performed and no application relevant analysis of its signal-to-noise performance has been done. Therefore, we perform here a detailed analysis of T-MOKE measurement capabilities using an effective polarization detection scheme by applying it to a series of especially challenging samples, in which the magneto-optical signal has been artificially reduced. Furthermore, we compare the performance of this methodology with conventional T-MOKE light intensity measurements. We observe a most significant improvement with a more than 30-fold increase in signal-to-noise ratio, which outperforms many of the specialized T-MOKE sample strategies that are being pursued [22, 25, 26, 28, 35], while being generally applicable at the same time.

Experiment

To allow for a direct comparison, two different T-MOKE detection methods have been used in this study. The first method is the conventional direct intensity T-MOKE measurement scheme, in which only p-polarized light is used and light intensity changes are monitored as the magnetic field is altered and causes a reversal of the sample magnetization. In contrast, the second method measures, as a function of the applied field, the magnetization state induced effective change in polarization by using incoming radiation that is a mixture of pure s- and p-polarized light. Given the fact that s-polarized light is not impacted by T-MOKE, while p-polarized light is changed in its amplitude and phase, the net polarization state of any mixed incoming polarization that is not pure s- or p-polarization will be changed by T-MOKE. Thus, for mixed incoming polarization states, T-MOKE measurements can be performed as polarization measurements [32, 34], and thus in principle can exhibit the high sensitivity that is traditionally associated with longitudinal and polar MOKE measurements only.

The setup that we used in our study of the polarization detection T-MOKE scheme is shown in figure 1(a). For our experiments, we utilized an ultra low noise laser [36] with λ=635 nm and an angle of incidence of 30º with respect to the surface normal [37]. The laser light first passes through a first quarter wave plate QWP1, then through the rotatable linear polarizer P1, and gets subsequently reflected by a sample that is placed inside the gap of an electromagnet. The reflected light beam then passes through a second rotatable quarter wave plate QWP2 and another rotatable linear polarizer P2, after which the transmitted light intensity is measured with a photo-detector. For our reference measurements that monitor the conventional p-polarized reflected light intensity T-MOKE, the same setup was utilized after QWP2 and P2 were removed and P1 was oriented in such a way, that pure p-polarized light was transmitted.

The function of QWP1 and P1 are simply the generation of a linearly polarized light beam, whose polarization orientation can be changed easily. The polarization axis itself is set by P1, and the function of QWP1 simply is the transformation of the linearly polarized light emitted by the laser into circular polarized light first. This has the advantage that independent from the P1 orientation, the light intensity at the sample is constant and all experiments are conducted at comparable light intensities. For an arbitrary incoming linear polarization, the phase shift in between s- and p-polarized reflectivities leads in the most general case to an elliptical polarization state in reflection, that is independent from magneto-optical effects. To compensate the purely optical ellipticity, QWP2 is aligned in such a way, that a purely linear polarization state is generated upon transmission through QWP2. The final optical element prior to the detector, i.e. the linear polarizer P2, is then aligned in such a way that it is nearly crossed to the polarization orientation that is transmitted by QWP2. Similar setups have been demonstrated to be very sensitive to small MOKE induced polarization changes and are routinely used for longitudinal and polar MOKE measurements [1, 5, 7].

In the alignment process, both QWP2 and P2 are rotated iteratively to minimize the signal at the photo detector. When the minimum signal is obtained, P2 is rotated a small angle away from that minimum intensity position, called the extinction position. In the experiments here, this angle from extinction was always set to 2º. In this configuration, one then follows the detected light intensity I as a function of the applied field H, which changes as the magnetization state of the sample changes. The observed intensity change ΔI in between inverted magnetization states is proportional to the MOKE induced ellipticity [7]. Specifically, we are monitoring here the fractional intensity change upon magnetization reversal $\Delta I/I$, defined as:

$$\frac{\Delta I}{I} = 2\,\frac{I(H)-I(-H)}{I(H)+I(-H)} \qquad (1),$$

which is the relevant signal of our effective polarization change T-MOKE experiment, and we compare it to the fractional intensity change upon magnetization reversal $\Delta I/I$ for purely p-polarized incoming light.

Prior to any T-MOKE measurement reported here, we first verified that the magnetic field was aligned perpendicular to the plane of incidence and in the plane of the sample, so that no longitudinal or polar MOKE would occur in our samples and thus interfere with our T-MOKE analysis. For this purpose, we conducted generalized magneto optical ellipsometry (GME) measurements that have the ability to separate the different MOKE signals [9] and allowed us to align the magnetization orientation to pure T-MOKE geometry to be better than 0.2º. We performed these GME measurements with the previously described setup after having QWP2 removed, which insured that the exact same plane of incidence and magnetic field orientation was used in all experiments.

Figure 1(b) shows some results obtained by using the effective polarization change T-MOKE detection scheme, namely the fractional intensity changes $\Delta I/I$ of two selected samples as a function of the incident polarization angle Θ_1. As expected, the $\Delta I/I$ signal approaches zero if the incoming polarization is approaching pure p-polarized light (Θ_1 = 0º) because no polarization change occurs in this case. Similarly, the signal vanishes upon approaching pure s-polarized light (Θ_1 = 90º), which is not affected by T-MOKE at all. When mixed s- and p-polarized light is used, however, a signal is clearly visible and reaches a maximum value for Θ_1 being around 45º. The exact position of the maximum depends on the specific sample and angle of incidence that is being used. Furthermore, it is noteworthy in figure 1(b) that the maximum magnitude of $\Delta I/I$ reaches nearly 2%, even though the magnetic sample is coated by 20 nm of Ag, which means that we can reach substantial signal levels, even for samples that do not exhibit very large magneto-optical effects.

In order to show the potential of the effective polarization T-MOKE method in comparison to conventional intensity T-MOKE measurements, we designed and fabricated a special set of samples that have a well defined, but weak T-MOKE effect. A schematic of the general sample structure is shown in the inset of figure 2. Si was used as a substrate, on which 10 nm of Cr were deposited as an adhesion layer. On top of the Cr, 100 nm of Co were deposited to generate a magnetic thin film sample that is far thicker than the optical skin depth, and thus represents bulk like optical behavior. On top of the Co film, a Ag layer of varying thickness t_{Ag} was deposited. To avoid surface oxidation, the Ag layer was covered with 10 nm SiO_2. All layers were deposited in direct sequence using sputter deposition [38], after calibrating the deposition rates for all materials. The purpose of these multilayer structures was to have samples with well-known and robust magnetic properties, but with very small magneto-optical signals. This is accomplished here by covering the thick Co layer with different thickness of Ag, so that most of the reflected light actually comes from the Ag layer, which does not carry a magneto-optical signal. Samples with 0, 20, 40, 60 and 80 nm Ag overcoat thickness were fabricated.

Given the fact that the MOKE-signal reduction depends now in a very sensitive manner on the accurate thickness calibration of the Ag-films, we were especially careful to establish accurate and repeatable deposition conditions for Ag and monitored those via X-Ray reflectivity (XRR) measurements. Figure 2 shows corresponding XRR data for a series of pure Ag films, whose thickness and thickness accuracy can be determined from the interference fringes. The curves in figure 2 show the normalized XRR intensity $\mathrm{Log}(I/I_{max})$ as a function of incidence angle ω. Utilizing these data, we verified that the error between the deposited Ag thickness and the nominal Ag thickness reported here was less than 1.2 nm for all our samples.

Results

Figure 3 shows a series of hysteresis loops, that we obtained on our samples under identical measurement conditions by using the two described T-MOKE detection schemes. Figure 3(a) represents examples of the hysteresis loops obtained via effective polarization change T-MOKE measurements, using an incoming polarization angle of Θ_1 = 45º for the entire data set, while the hysteresis loops obtained via conventional intensity T-MOKE measurements are presented in figure 3(b) [39]. From this figure one can see that we achieved a high signal-to-noise ratio (SNR) for both methods for the uncovered Co-film, even if the effective polarization change T-MOKE measurements produce a $\Delta I/I$ signal that is about 20 times higher than that for the conventional intensity change T-MOKE.

As intended, the magneto-optical signals of the samples with Ag overcoats are substantially reduced. As we can see from figure 3, for both methods the obtained $\Delta I/I$ signals decrease with an increase of the Ag overcoat thickness, and simultaneously the SNRs of the measurements deteriorate. Due to this signal and SNR reduction, we could not use the conventional intensity T-MOKE type methodology to successfully record hysteresis loops of samples with 60 nm or 80 nm of Ag overcoat. So, for these two samples in particular the advantage of the effective polarization type T-MOKE measurement is most obvious, because with this methodology, we were actually able to measure their hysteresis loops, even if the 80 nm coated sample exhibits a T-MOKE signal that was only 1/600 of the signal for the uncoated Co-sample. The key reason for this improved performance of the polarization measurement is the fact that the $\Delta I/I$ signal is enhanced by an average factor of more than 30 due to the fact that most of the reflected light that does not carry T-MOKE information is separated out by the polarization optics and does not enter the photo detector. This signal enhancement can be very clearly seen in figure 4(a), where the $\Delta I/I$ signal is plotted vs. the Ag coating thickness for both T-MOKE measurement methods. Here, a consistent signal enhancement is obvious for the effective polarization measurement, which furthermore translates to a very similar enhancement of the SNR as shown in figure 4(b). This substantial signal and SNR enhancement then enabled us to also measure with the effective polarization methodology the far smaller T-MOKE effects of the samples with the thickest Ag coating, for which the conventional direct intensity measurement fails.

With respect to the SNR improvement, it is worthwhile to notice in figure 3, that for comparable $\Delta I/I$ amplitudes (as, for instance, the conventional direct intensity change T-MOKE for the 20 nm Ag overcoat sample vs. the effective polarization change T-MOKE for the 60 nm Ag overcoat sample) we find a slightly lower SNR value for the polarization sensitive detection, because the conventional intensity T-MOKE measurement is conducted on an overall higher light intensity level I. However, this is relatively small secondary effect that does not relevantly counteract the huge $\Delta I/I$ amplitude increase that is facilitated by the effective polarization methodology. Thus, the $\Delta I/I$ signal enhancement found in figure 4(a) leads to an almost identical SNR increase, as shown in figure 4(b), if one compares the two measurement approaches.

Figure 4(a) also shows clearly that $\Delta I/I$ signal follows the expected exponential decrease with Ag overcoat thickness, for which we have determined the information depth $\delta = 12.35 \pm 0.45$ nm as the relevant falloff length. This falloff length corresponds to half of the skin depth, considering the fact that the light entering the metallic Ag overcoat is damped and shifted in its phase, generates a certain Kerr amplitude at the Co-film interface at depth t_{Ag}, which then has to travel back to the surface, thus being absorbed and shifted again by the same amount [40]. Thus, the results in figure 4 tell us that with effective polarization T-MOKE, we are capable of measuring magnetic properties below the surface, even below six times the information depth δ, where the signal has decreased to almost 1/1000 of the signal of an uncoated Co-film.

Discussion and conclusions

Our comparative experiments here demonstrate that with an appropriate detection system based on an effective polarization measurement scheme, in which the light amplitude that does not carry magnetic information is substantially reduced, we are able to gain a most significant signal and SNR increase, which is about 30-fold for the specific conditions used in this study.

While the effective polarization T-MOKE measurement scheme shows relevant improvements over the conventional direct intensity T-MOKE measurements already for uncoated Co-films that exhibit a strong signal, the true potential of this methodology becomes obvious, when applied to samples with very small signals, which we produced by coating similar Co samples with Ag films of precisely defined thickness. On these samples, we were able to measure signals that are far higher if compared to conventional direct intensity T-MOKE measurements. This increase in signal and the associated increase in SNR also enabled us to measure magneto-optical signals and hysteresis loops for samples that were covered by more than 40 nm of Ag overcoat, for which conventional T-MOKE measurements failed due to the lack of sensitivity.

Furthermore, we demonstrated that the T-MOKE ellipticity is a function of the incoming light orientation, which reaches a maximum near at Θ_1=45º, as can be seen in figure 1(b). While it is clear that the T-MOKE polarization signal has to always vanish for Θ_1 = 0º and Θ_1 = 90º, given that there is no polarization conversion (s to p or vice versa) occurring in the sample for T-MOKE, the exact position of the maximum depends of the specific amplitudes and phases of the s- and p-polarized reflectivities.

In our experiments the P2 angle was always rotated by the same angle, i.e. 2º away from the angle of extinction and was not individually optimized. This was done for the purpose of assembling easily comparable results for all samples and incoming polarizations. Otherwise, the comparative $\Delta I/I$ plots in figures 1 and 4 would not have been possible and the general behavior would not have been easily transparent. Nevertheless, the observed improvements for the measured signals and SNRs are most substantial, even if they are not actually optimized yet. Thus, by identifying individually optimized settings for the polarization optic elements, the ultimate detection limit can be improved even further, making the effective polarization detection T-MOKE yet more attractive.

Acknowledgment

We acknowledge support from the Basque Government under the Elkartek program, project No. KK-2016/00025, from the Spanish Ministry of economy and competitiveness under Project No. FIS2015-64519-R (MINECO/FEDER). P.R. acknowledges Obra Social "la Caixa" for her Ph.D. fellowship and L.F. acknowledges support from the Predoctoral program of the Basque Government through the Grant No. PRE_2015_2_0126.

Figures

Figure 1: (a) Experimental setup for polarization detection T-MOKE analysis consisting of laser source, first quarter wave plate (QWP1), first polarizer (P1), second quarter wave plate (QWP2), second polarizer (P2) and detector. (b) T-MOKE (ΔI/I) signal, measured with the setup shown in (a), as a function of incident polarization orientation Θ_1, for Co-film samples covered with 20 nm of Ag overcoat (◆) and 40 nm of Ag overcoat (●).

Figure 2: Normalized XRR intensity Log (I/I_{max}) vs. incidence angle ω obtained for pure Ag film reference samples of thickness t_{Ag} grown by means of sputter deposition at room temperature. The complete test samples for the magneto-optical study have the structure shown in the inset.

Figure 3: Experimental hysteresis loops obtained with (a) the effective polarization change T-MOKE detection method and with (b) the conventional direct intensity T-MOKE detection for Co-film samples with 0, 20, 40, 60 and 80 nm of Ag overcoat.

Figure 4: (a) ΔI/I signal and (b) signal-to-noise ratio (SNR) as a function of Ag overcoat thickness for effective polarization change T-MOKE measurements (■) and conventional direct intensity T-MOKE measurements (●). The solid lines correspond to least-squares fits of an exponential decrease $S = S_0 \exp(-t_{Ag}/\delta))$ in each case, for which $\delta = 12.35 \pm 0.45$ nm was determined from the signal vs. t_{Ag} behavior of the effective polarization change T-MOKE. The dashed horizontal lines indicate the detection limits of our setups.

References

[1] See: Z. Q. Qiu and S. D. Bader, Surface magneto-optic Kerr effect (SMOKE), *J. Magn. Magn. Mater.*, vol. 200, no. 1–3, pp. 664–678, 1999 and reference therein.

[2] P. N. Argyres, Theory of the Faraday and Kerr Effects in Ferromagnetics, *Phys. Rev.*, vol. 97, no. 2, pp. 334–345, Jan. 1955.

[3] R. P. Hunt, Magneto-optic scattering from thin solid films, *J. Appl. Phys.*, vol. 38, no. 4, pp. 1652–1671, 1967.

[4] M. Freiser, A survey of magnetooptic effects, *IEEE Transactions on Magnetics*, vol. 4, no. 2. pp. 152–161, 1968.

[5] E. R. Moog and S. D. Bader, Smoke signals from ferromagnetic monolayers: p(1×1) Fe/Au(100), *Superlattices Microstruct.*, vol. 1, no. 6, pp. 543–552, 1985.

[6] Z. Qiu, J. Pearson, and S. Bader, Asymmetry of the spin reorientation transition in ultrathin Fe films and wedges grown on Ag(100)., *Phys. Rev. Lett.*, vol. 70, no. 7, pp. 1006–1009, Feb. 1993.

[7] A. Berger, S. Knappmann, and H. P. Oepen, Magneto-optical Kerr effect study of ac susceptibilities in ultrathin cobalt films, *Journal of Applied Physics*, vol. 75, no. 10, pp. 5598–5600, 1994.

[8] C.-Y. You and S.-C. Shin, Generalized analytic formulae for magneto-optical Kerr effects, *J. Appl. Phys.*, vol. 84, no. 1, p. 541, 1998.

[9] A. Berger and M. R. Pufall, Quantitative vector magnetometry using generalized magneto-optical ellipsometry, *J. Appl. Phys.*, vol. 85, no. 8, pp. 4583–4585, 1999.

[10] A. Carl and D. Weller, Oscillatory paramagnetic magneto-optical Kerr effect in Ru wedges on Co., *Phys. Rev. Lett.*, vol. 74, no. 1, pp. 190–193, Jan. 1995.

[11] M. Grimsditch and P. Vavassori, The diffracted magneto-optic Kerr effect: what does it tell you?, *J. Phys. Condens. Matter*, vol. 16, no. 9, pp. R275–R294, 2004.

[12] J. McCord, Progress in magnetic domain observation by advanced magneto-optical microscopy, *J. Phys. D. Appl. Phys.*, vol. 48, no. 33, p. 333001, Aug. 2015.

[13] J. A. Arregi, P. Riego, and A. Berger, What is the longitudinal magneto-optical Kerr effect?, *J. Phys. D. Appl. Phys.*, vol. 50, no. 3, p. 03LT01, 2017.

[14] R. Carey and B. W. J. Thomas, The theory of the Voigt effect in ferromagnetic materials, *J. Phys. D. Appl. Phys.*, vol. 7, no. 17, pp. 2362–2368, 1974.

[15] A. Hubert and G. Traeger, Magneto-optical sensitivity functions of thin-film systems, *J. Magn. Magn. Mater.*, vol. 124, no. 1–2, pp. 185–202, 1993.

[16] K. Postava, H. Jaffres, A. Schuhl, F. Nguyen Van Dau, M. Goiran, and A. R. Fert, Linear and quadratic magneto-optical measurements of the spin reorientation in epitaxial Fe films on MgO, *J. Magn. Magn. Mater.*, vol. 172, no. 3, pp. 199–208, 1997.

[17] R. M. Osgood III, S. D. Bader, B. M. Clemens, R. L. White, and H. Matsuyama, Second-order magneto-optic effects in anisotropic thin films, *J. Magn. Magn. Mater.*, vol. 182, no. 3, pp. 297–323, 1998.

[18] A. K. Zvezdin and V. A. Kotov, *Modern magnetooptics and magnetooptical materials*. CRC Press, 1997.

[19] S. Tsunashima, Magneto-optical recording, *J. Phys. D. Appl. Phys.*, vol. 34, no. 17, pp. R87–R102, Sep. 2001.

[20] M. Donolato *et al.*, On-chip manipulation of protein-coated magnetic beads via domain-wall conduits, *Adv. Mater.*, vol. 22, no. 24, pp. 2706–2710, 2010.

[21] Y. Shoji, Y. Shirato, and T. Mizumoto, Silicon Mach–Zehnder interferometer optical isolator having 8 nm bandwidth for over 20 dB isolation, *Jpn. J. Appl. Phys.*, vol. 53, no. 2, p. 22202, Feb. 2014.

[22] L. E. Kreilkamp *et al.*, Waveguide-plasmon polaritons enhance transverse magneto-optical kerr effect, *Phys. Rev. X*, vol. 3, no. 4, pp. 1–7, 2014.

[23] S. U. Jen and K. C. Chen, Enhancement of polar Kerr effect by forming Au nanoparticles on Ni surface, *J. Appl. Phys.*, vol. 97, no. 10, pp. 15–18, 2005.

[24] V. I. Belotelov *et al.*, Enhanced magneto-optical effects in magnetoplasmonic crystals., *Nat. Nanotechnol.*, vol. 6, no. 6, pp. 370–376, 2011.

[25] M. Tejedor, A. Fernández, and M. A. Cerdeira, Enhancement of the transverse Kerr magneto-optic effect by multiple reflections, *Rev. Sci.*

Instruments 69, vol. 4000, no. 1998, pp. 17–19, 2011.

[26] R. P. Hunt, Contrast enhancement of the transverse Kerr effect, *J. Appl. Phys.*, vol. 38, no. 3, pp. 1215–1216, 1967.

[27] Z. Q. Qiu and S. D. Bader, Surface magneto-optic Kerr effect, *Rev. Sci. Instrum.*, vol. 71, no. 3, p. 1243, 2000.

[28] J. A. Girón-Sedas, J. R. Mejia-Salazar, E. Moncada-Villa, and N. Porras-Montenegro, Enhancement of the transverse magneto-optical Kerr effect via resonant tunneling in trilayers containing magneto-optical metals, *Appl. Phys. Lett.*, vol. 109, no. 3, pp. 1–5, 2016.

[29] V. I. Belotelov, D. A. Bykov, L. L. Doskolovich, A. N. Kalish, and A. K. Zvezdin, Giant transversal Kerr effect in magneto-plasmonic heterostructures: The scattering-matrix method, *J. Exp. Theor. Phys.*, vol. 110, no. 5, pp. 816–824, May 2010.

[30] A. A. Grunin, A. G. Zhdanov, A. A. Ezhov, E. A. Ganshina, and A. A. Fedyanin, Surface-plasmon-induced enhancement of magneto-optical Kerr effect in all-nickel subwavelength nanogratings, *Appl. Phys. Lett.*, vol. 97, no. 26, p. 261908, 2010.

[31] D. M. Newman, M. L. Wears, R. J. Matelon, and I. R. Hooper, Magneto-optic behaviour in the presence of surface plasmons, *J. Phys. Condens. Matter*, vol. 20, no. 34, p. 345230, Aug. 2008.

[32] A. Berger, A. W. Pang, and H. Hopster, Magnetic reorientation transition in epitaxial Gd-films, *J. Magn. Magn. Mater.*, vol. 137, no. 1–2, pp. L1–L5, 1994.

[33] A. Berger, A. W. Pang, and H. Hopster, Magnetic reorientation transition of Gd(0001)/W(110) films, *Phys. Rev. B*, vol. 52, no. 2, pp. 1078–1089, 1995.

[34] D. A. Allwood, P. R. Seem, S. Basu, P. W. Fry, U. J. Gibson, and R. P. Cowburn, Over 40% transverse Kerr effect from Ni[sub 80]Fe[sub 20], *Appl. Phys. Lett.*, vol. 92, no. 7, p. 72503, 2008.

[35] L. G. C. Melo, A. D. Santos, L. M. Alvarez-Prado, and Y. Souche, Optimization of the TMOKE response using the ATR configuration, *J. Magn. Magn. Mater.*, vol. 310, no. 2 SUPPL. PART 3, pp. 2006–2008, 2007.

[36] The laser used in these experiments is an ultra low noise laser with RMS noise of 0.06%, λ=635 nm, a polarization ratio > 100:1, and an output power of 5 mW.

[37] The T-MOKE signal is actually larger at a larger angles of incidence. However, the purpose of this study was to demonstrate the capability of our methodology to measure very small T-MOKE signals. Therefore, we did not optimize the angle of incidence to achieve the largest possible T-MOKE effect.

[38] Details of our sample fabrication using sputter deposition can be found in: Appl. Phys. Lett. 103, 102410 (2013) or Journal of Applied Physics 115, 083912 (2014).

[39] The data in figure 3 were measured by using an acquisition time of 0.6 seconds per data point for the samples with 0, 20, 40, 60 nm of Ag overcoat thickness and 3 seconds per data point for the sample with 80 nm of Ag overcoat (for both detection schemes).

[40] G. Traeger, L. Wenzel, and A. Hubert, Computer experiments on the information depth and the figure of merit in magnetooptics, *Phys. status solidi*, vol. 131, no. 1, pp. 201–227, 1992.

Figure 1

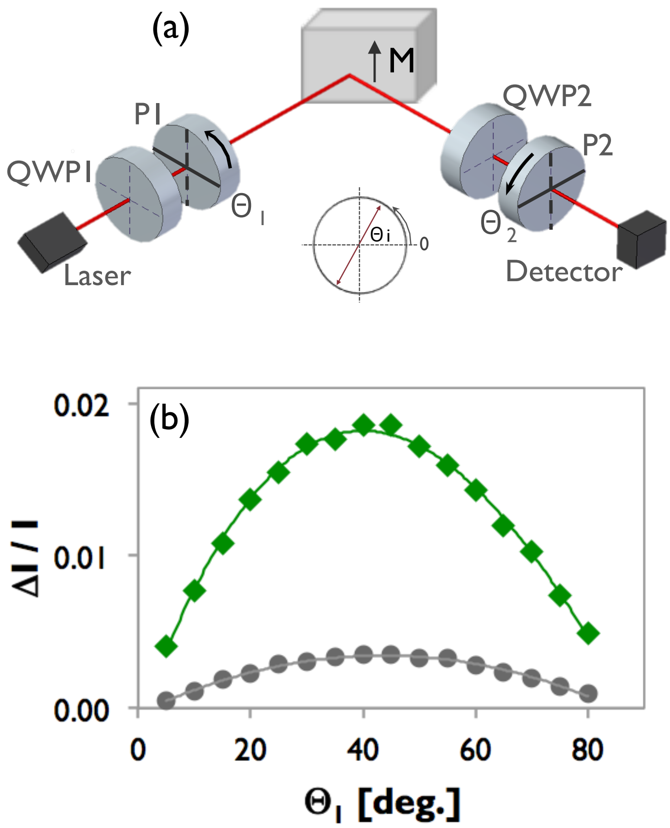
(a)
M
QWP2
P1
P2
QWP1
Θ 1
Θi
0
Θ 2
Laser
Detector
(b)
0.02
0.01
0.00
ΔI / I
0
20
40
60
80
Θ1 [deg.]

Figure 2

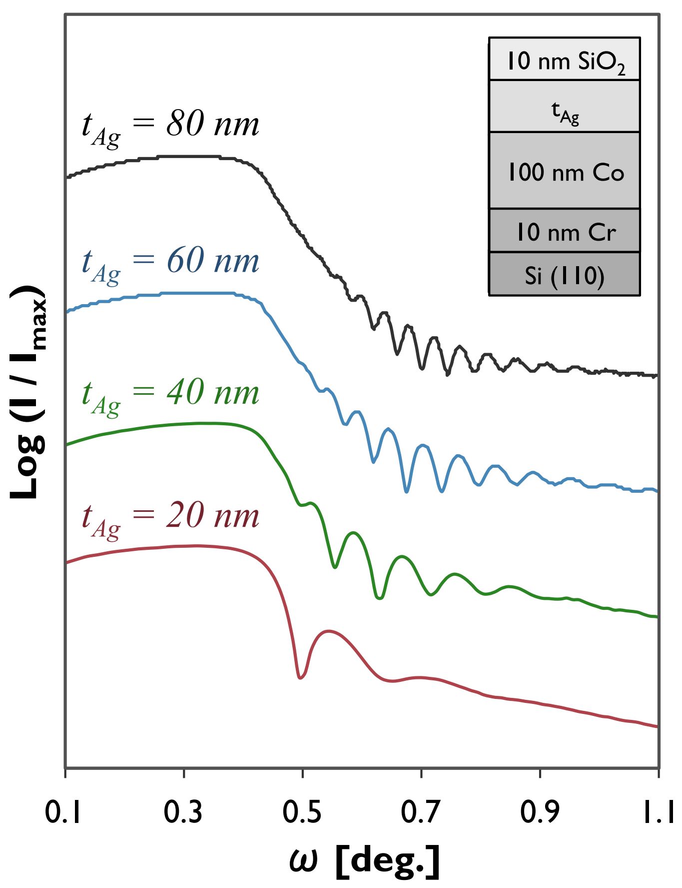

10 nm SiO2
tAg
100 nm Co
10 nm Cr
Si (110)
tAg = 80 nm
tAg = 60 nm
tAg = 40 nm
tAg = 20 nm
Log (I / Imax)
0.1
0.3
0.5
0.7
0.9
1.1
ω [deg.]

Figure 3

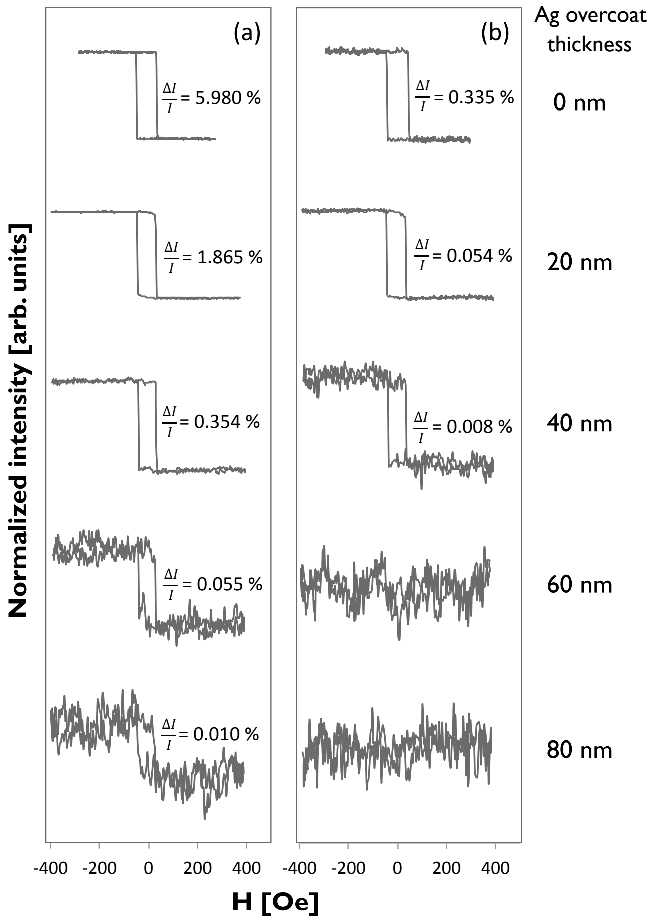
(a)
(b)
Ag overcoat thickness
$\frac{\Delta I}{I}$ = 5.980 %
$\frac{\Delta I}{I}$ = 0.335 %
0 nm
$\frac{\Delta I}{I}$ = 1.865 %
$\frac{\Delta I}{I}$ = 0.054 %
20 nm
$\frac{\Delta I}{I}$ = 0.354 %
$\frac{\Delta I}{I}$ = 0.008 %
40 nm
$\frac{\Delta I}{I}$ = 0.055 %
60 nm
$\frac{\Delta I}{I}$ = 0.010 %
80 nm
Normalized intensity [arb. units]
-400 -200 0 200 400
-400 -200 0 200 400
H [Oe]

Figure 4